

# Dynamic Performance Research on Reversing Valve of Hydraulic Breaker\*

Guoping Yang<sup>1</sup>, Yubao Chen<sup>2</sup>, Bo Chen<sup>1</sup>

<sup>1</sup>College of Automotive Engineering, Shanghai University of Engineering and Science, Shanghai, China

<sup>2</sup>Department of Industrial & Manufacturing Systems Engineering, University of Michigan-Dearborn, Dearborn, USA  
Email: ygpljyl@163.com

Received August 2, 2012; revised September 1, 2012; accepted September 17, 2012

## ABSTRACT

The structure and operational principle on a new type reversing valve of hydraulic breaker are introduced. The nonlinear mathematic model and simulation model of the new type reversing valve are built. The dynamic simulation research of the new type reversing valve is conducted. The effects of the system parameters on the working performance are researched systematically and deeply. The regular understanding on the motion of the reversing valve is obtained, which provides theoretical basis for the innovation and manufacturing of a new generation of hydraulic breaker reversing valve.

**Keywords:** Hydraulic Breaker; Reversing Valve; Dynamic Performance; Nonlinear Mathematic Model; Computer Simulation

## 1. Introduction

Hydraulic breakers are used widely now in construction fields such as road, civil engineering, port, and mines. The breakers work on the principle of hydraulics, applying Pascal's Law, high pressure oil and nitrogen gas drive the piston to move back and forth, striking the rod through which impact power is transmitted to the working objection. For most present impactors, the impact energy and frequency cannot be adjusted steplessly. In recent years, by making a systematic and deep study, a controlled hydraulic breaker whose parameters can be adjusted continually is developed [1-10]. In this paper, the author makes computer simulation research on the controlled hydraulic breaker reversing valve.

## 2. Structure and Operating Principle of the New Type Reversing Valve

### 2.1. Structure of the New Type Reversing Valve

The new type reversing valve is a combined control valve (Figures 1 and 3) which consists of the pilot valve and directional control valve. The new type reversing valve mainly consists of directional control valve core 3, damping 4, spring 5 and pilot valve core 13, spring 12, seat 14. The actual photo of the new type reversing valve is shown in Figure 2.

\*This project is supported by National Natural Science Foundation of China (Grant No. 50975169).

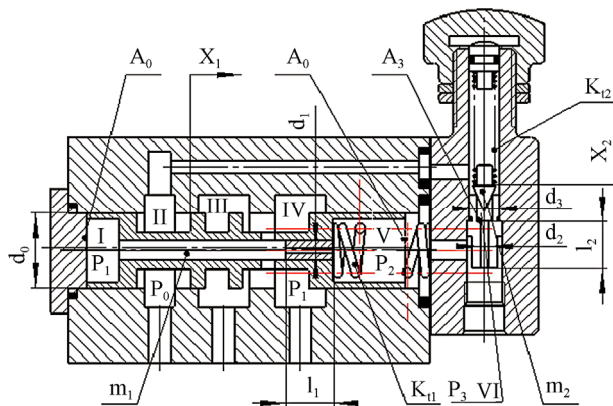


Figure 1. Structure of the new type reversing valve.

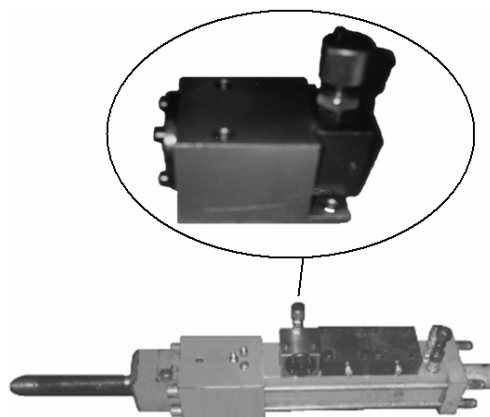
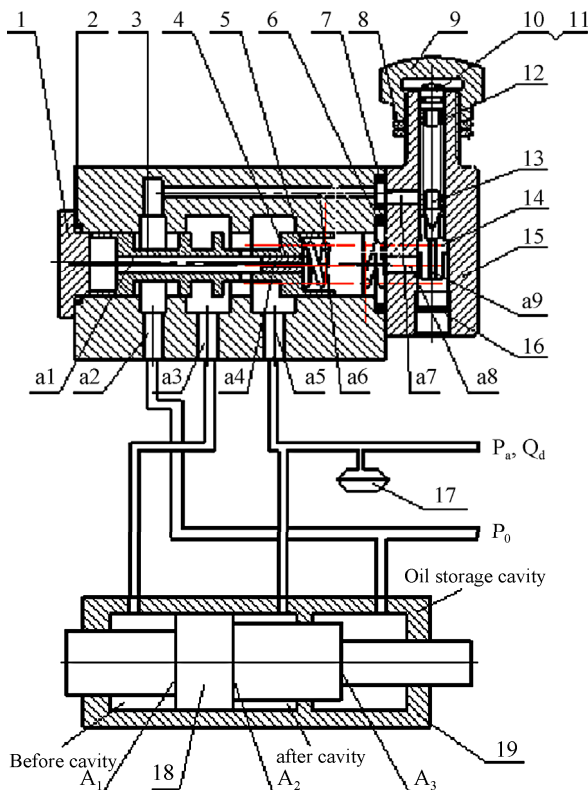


Figure 2. Picture of the new type reversing valve.

## 2.2. Operational Principle of the New Type Reversing Valve

The new type reversing valve is the direction-changing mechanism of the pressure feedback hydraulic impactor. When explaining the operational principle of the new pilot reversing valve, the function of the piston and high pressure accumulator of the pressure feedback hydraulic impactor must be taken into consideration. The operational principle of the new type reversing valve is shown in **Figure 3**.

As shown in **Figures 1 and 3**, the directional valve core is on the left under the action of the spring prepressure after the assembly is finished. Inside the directional valve, the chamber III and IV are connected. At the moment, one part of the high-pressure oil from the oil pump directly flows into the back chamber of the piston, the other first flows into the chamber IV of the directional valve via the oil duct a6, then flows into the chamber III via the valve orifice, and then flows into the front chamber of the piston via the oil duct a3, which makes the high-pressure oil flow into the front and back chamber at the same time. At this moment,  $P_1 = P_2 = P_d$ .  $A_1$  is the effective action area of the front chamber of the piston, and  $A_2$  is the effective action area of the back chamber of the piston.  $A_1$  is larger than  $A_2$  and the return oil chamber is connected with the reservoir, so  $P_1A_1 > P_2A_2 + P_0A_3$ .



**Figure 3.** Operational principle of the new type reversing valve.

Therefore, the piston makes return accelerated motion under the action of the differential pressure. With the piston accelerated movement towards the right, the high-pressure accumulator 17 fills in oil fluid and the system pressure  $P_d$  raises. When  $P_d$  rises to a certain value, the pilot poppet valve 13 opens, the oil flows back to the reservoir via the oil duct a5, directional valve center orifice a1, damping orifice a4, oil chamber V, oil duct a8, damping orifice a9 in poppet valve seat, oil duct a7, a6 and a2. There is a pressure difference between the left and right chambers of the directional valve core due to damping orifice a4. When the right force caused by the differential pressure exceeds the force of directional valve spring, the directional valve core moves toward the right, the chamber II and III of directional valve are connected, and then the piston begins return deceleration or impact travel. At the moment, one part of oil fluid in the piston front chamber flows into the return oil chamber via the oil duct a2 and a3. The other flows back to the reservoir. At the same time, the piston does accelerate movement towards the left, the system pressure gradually decreases. When the system pressure decreases to a certain value, the pilot poppet valve closes. The directional valve resets under the action of spring and enters into the return travel working condition of the next cycle [1-5].

## 3. Symbolic Meaning and Reference Value

The symbolic meaning and parameters which are ascertained according to the structural dimension and working conditions of the new type reversing valve are shown in Appendix.

## 4. Foundation of Mathematical Mode

Based on working principle, when the system pressure increases to the setting pressure of the pilot valve, the directional valve changes direction in the return travel. When the system pressure decreases to the setting pressure of the pilot valve, the directional valve changes direction in the impact travel. In the case that the pre-compression of the press-adjusting spring of the pilot valve is certain, the time of return and impact travel is directly decided by the system impact pressure  $P_1$  which accordingly decides the impact energy of the hydraulic impactor and whether it can work normally or not. Hence, in order to study the dynamic performance of the reversing valve, we put a flow signal of square-wave step into the system, which makes the system pressure increase from zero to the setting pressure of the pilot valve and then decrease from the setting pressure to zero after one cycle time  $T$ .

Here, the force balance of the directional valve core and pilot valve core and the flow continuity relationship when oil flows through the directional valve and pilot

valve are mainly considered. The gravity of the valve core and the coulomb friction are ignored for simplifying the problem. The dynamic process of the reversing valve is only considered and the throttling effect of the directional valve orifice is not considered. According to **Figures 1** and **3**, the nonlinear mathematical model is built as follows [6].

1) The flow continuity equation of the directional valve orifice:

$$Q_s = \frac{1}{C_{e1}} \cdot \frac{\pi d_1^4}{128 \mu l_1} (p_1 - p_2) + \frac{V_1}{K} \cdot \frac{dp_1}{dt} + A_0 \frac{dx_1}{dt} \quad (1)$$

2) The flow continuity equation of the back chamber of the directional valve:

$$\frac{1}{C_{e2}} \cdot \frac{\pi d_2^4}{128 \mu l_2} \cdot (p_2 - p_3) = \frac{1}{C_{e1}} \cdot \frac{\pi d_1^4}{128 \mu l_1} \cdot (p_1 - p_2) - \frac{V_1}{K} \cdot \frac{dp_2}{dt} + A_0 \frac{dx_1}{dt} \quad (2)$$

3) The flow continuity equation of the pilot valve:

$$\frac{1}{C_{e2}} \cdot \frac{\pi d_2^4}{128 \mu l_2} \cdot (p_2 - p_3) = C_{d2} \pi d_3 \sin \alpha_2 \sqrt{\frac{2}{\rho} p_3 \cdot x_2} + A_3 \frac{dx_2}{dt} + \frac{V_3}{K} \cdot \frac{dp_3}{dt} \quad (3)$$

4) The force balance equation of the directional valve core:

$$A_0 p_1 - A_0 p_2 = m_1 \frac{d^2 x_1}{dt^2} + B_1 \frac{dx_1}{dt} + k_{t1} (x_1 + x_{t1}) \quad (4)$$

5) The force balance equation of the pilot core:

$$A_3 p_3 = m_2 \frac{d^2 x_2}{dt^2} + B_2 \frac{dx_2}{dt} + k_{t2} (x_2 + x_{t2}) + C_{d1} C_{v1} \pi d_3 \sin 2\alpha_1 \cdot x_2 p_3 - L_2 C_{d1} \pi d_3 \sin \alpha_{12} \sqrt{2\rho} p_3 \frac{dx_2}{dt} \quad (5)$$

The above five equations are the basic form of the mathematical mode describing the dynamic characteristic of the distribution valve.

The steady-state fluid force coefficient of the pilot valve is defined by

$$C_1 = C_{d1} C_{v1} \pi d_3 \sin 2\alpha_1$$

The instantaneous-state fluid force coefficient of the pilot valve is defined by

$$C_2 = L_1 C_{d1} C_{v1} \pi d_3 \sin \alpha_1 \sqrt{2\rho}$$

The damping orifice fluid resistance of the damping orifice of the directional valve is defined by

$$R_1 = C_{e1} \cdot \frac{128 \mu l_1}{\pi d_1^4}$$

The damping orifice fluid resistance of the damping orifice of the pilot valve is defined by

$$R_2 = C_{e2} \cdot \frac{128 \mu l_2}{\pi d_2^4}$$

The outflow coefficient of the pilot valve orifice is defined by

$$K_1 = C_{d1} \pi d_3 \sin \alpha \sqrt{\frac{2}{\rho}}$$

Suppose:

$$y_1 = p_1, y_2 = p_2, y_3 = p_3, y_4 = x_1, y_5 = \dot{x}_1, y_6 = x_2, y_7 = \dot{x}_2$$

And define:

$$b_1 = \frac{K}{V_1}, b_2 = \frac{K}{V_2}, b_3 = \frac{K}{V_3}$$

$$F_{10} = k_{t1} x_{t1}, F_{20} = k_{t2} x_{t2}$$

$$S_1 = b_1 Q_s, S_2 = \frac{F_{10}}{m_1}, S_3 = \frac{F_{20}}{m_2}$$

$$a_{11} = a_{12} = \frac{b_1}{R_1}, a_{15} = b_1 A_1$$

$$a_{21} = \frac{b_2}{R_1}, a_{22} = \left( \frac{1}{R_1} + \frac{1}{R_2} \right) b_2,$$

$$a_{23} = \frac{b_2}{R_2}, a_{25} = b_2 A_2$$

$$a_{32} = a_{33} = \frac{b_3}{R_2}, a_{36} = b_3 K_2 \sqrt{y_3},$$

$$a_{37} = b_3 A_2, a_{51} = \frac{A_1}{m_1}$$

$$a_{52} = \frac{A_2}{m_1}, a_{54} = \frac{k_{t1}}{m_1}, a_{55} = \frac{B_1}{m_1}$$

$$a_{73} = \frac{A_3}{m_2}, a_{76} = \frac{k_{t2}}{m_2}, a_{77} = \frac{B_2}{m_2}$$

Substituting Equations (1)-(5), the following state equations can be obtained:

$$\begin{cases} \dot{y}_1 = -a_{11} y_1 + a_{12} y_2 - a_{15} y_5 + S_1 \\ \dot{y}_2 = a_{21} y_1 - a_{22} y_2 + a_{23} y_3 + a_{25} y_5 \\ \dot{y}_3 = a_{32} y_2 - a_{33} y_3 - a_{36} y_6 - a_{37} y_7 \\ \dot{y}_4 = y_5 \\ \dot{y}_5 = a_{51} y_1 - a_{52} y_2 - a_{54} y_4 - a_{55} y_5 - S_2 \\ \dot{y}_6 = y_7 \\ \dot{y}_7 = a_{73} y_3 - a_{76} y_6 - a_{77} y_7 - S_3 \end{cases}$$

## 5. Simulation Results and Analysis

A flow signal of square-wave step is input into the distribution valve. The system pressure will dynamically rise from zero to the setting pressure of the pilot valve and then the system pressure decreases from the setting pressure to zero after one cycle  $T$ . The actual displacement response of the pilot valve and the directional valve is shown in **Figure 4**. The response consists of three parts, the first part is the response of positive step, the second part is steady-state area and the third part is the response of negative step. In the region of positive step response,  $t_{yz}$  is the delay time when the pilot valve opens or the directional valve changes direction,  $t_{rz}$  is the peak time when the pilot valve opens or the directional valve changes direction,  $t_{sz}$  is the transition time when the pilot valve opens or the directional valve changes direction. In the region of negative step response,  $t_{yf}$  is the delay time when the pilot valve closes or the directional valve resets,  $t_{rf}$  is the peak time when the pilot valve closes or the directional valve resets,  $t_{sf}$  is the transition time when the pilot valve closes or the directional valve resets [7].

In the process of the negative step response, the pilot valve core gets the mechanical limit of the pilot valve seat and the directional valve core gets the mechanical limit of the directional valve body, so the overshoot phenomenon does not appear and one or two tiny rebound waves which do not affect the characteristic of the distribution valve may only appear. Thus, the positive step response is only studied. Videlicet, the dynamic characteristic when the pilot valve opens or the directional valve changes direction in the return travel is studied. The simulation results are as follows.

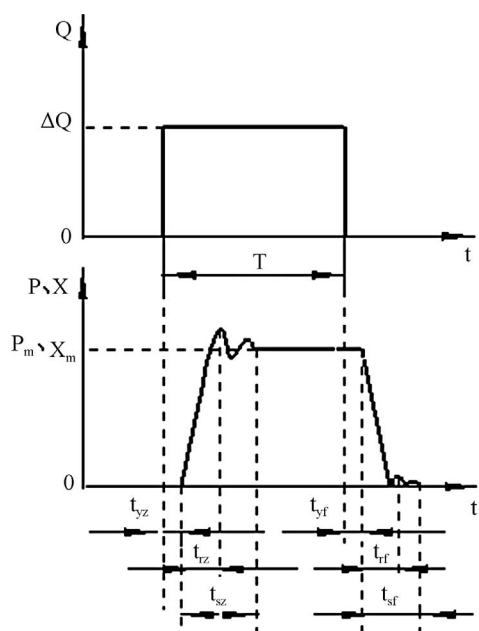


Figure 4. Step response curves of the distribution valve.

1) The dynamic characteristics of the valve at the different setting pressure and the same step flow.

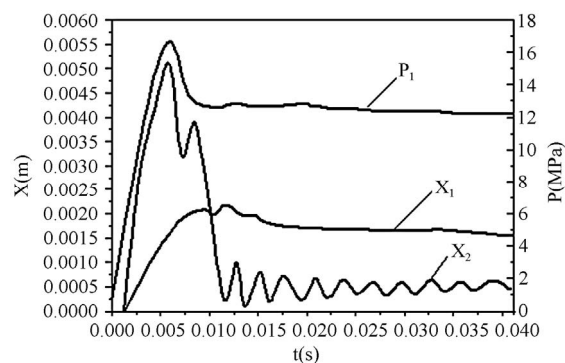
**Figures 5(a) and (b)** show the dynamic response curve when the setting pressure  $P^*$  is 11 MPa and 15 MPa, the initial oil pressure  $P_0$  is 0.8 MPa, the step flow  $\Delta Q$  is 40 l/min. The conclusions are as follows:

a) The valve is stable under the conditions of the existing structural parameters. The stability of the pressure value and the directional valve core displacement  $X_1$  is good. The oscillation of the pilot valve is convergent. The amplitude increases with the decrease of the setting pressure. When  $P^*$  is 11 MPa, the amplitude tends equivalent. This shows that considering from the point of the dynamic characteristic; its performance will be degraded when the distribution valve works under the condition which is far away from the designed situation.

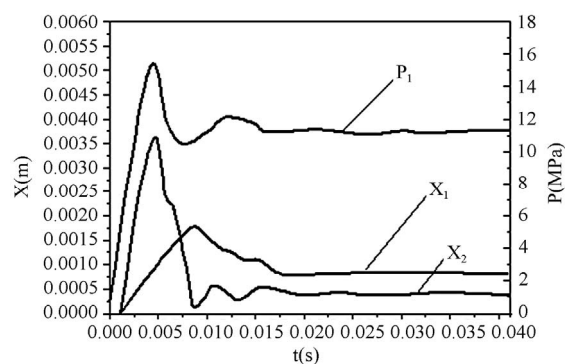
b) The peak value of  $P_1$  decreases with the decrease of the setting pressure, but its overshoot  $\Delta P_1$  is nearly constant which shows the pressure overshoot has nothing to do with the steady-state pressure.

c) Under the current parameters,  $\Delta P_1$  is 12 MPa, the peak time  $t_{rz}$  is 0.003 s to 0.004 s, the transition process time  $t_{sz}$  is about 0.03 s, which shows that the time-domain dynamic quality index of the valve is satisfying.

2) The dynamic characteristics at the same setting pressure, the same step flow and the different initial conditions.



(a)



(b)

Figure 5. Simulation curves one.

Figures 6(a) and (b) show the dynamic response curve when the initial oil pressure  $P_0$  is respectively 0.2 MPa and 0.6 MPa, the setting pressure  $P^*$  is 14 MPa, the step flow  $\Delta Q$  is 40 l/min. It is obvious in Figure 6 that the valve is stable no matter the initial conditions, the excessive pressure adjustment  $\Delta P_1$  doesn't change with the initial conditions, the peak and rise time of  $P_1$  basically does not change with the initial conditions.

3) The dynamic characteristics at the same setting pressure and different step flow.

The response curves (Figures 7(a)-(c)) of the inlet port oil pressure, the pressure  $P^*$  is 15 MPa and the step flow  $\Delta Q$  is 40, 25, 15 l/min. By comparison, the conclusions are as follows:

a) The pressure overshoot  $\Delta P_1$  is obviously affected by the step flow. The smaller the overflow, the smaller the overshoot.

b) The pressure rise time, peak time and transition process time increase with the decrease of the overflow quantity.

c) The changes of the overflow quantity within a certain range nearly affect the stability of the valve.

4) Effects of the directional valve core damping orifice on the distribution valve dynamic characteristics.

The curves shown in Figures 8(a)-(c) are respectively the characteristic curves of the pilot valve core and directional valve core displacement when the diameter of the directional valve damping orifice is 0.15 cm (the thick curve in Figure), 0.12 cm (the middle-thick curve in Figure), 0.10 cm (the thin curve) under the conditions that the initial oil pressure is 0.8 MPa, the setting pressure is 15 MPa and the step flow  $\Delta Q$  is 40 l/min.

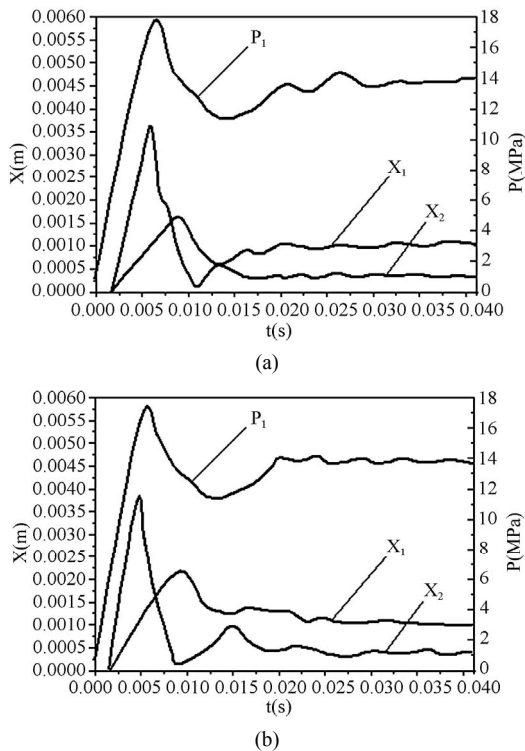


Figure 6. Simulation curves two.

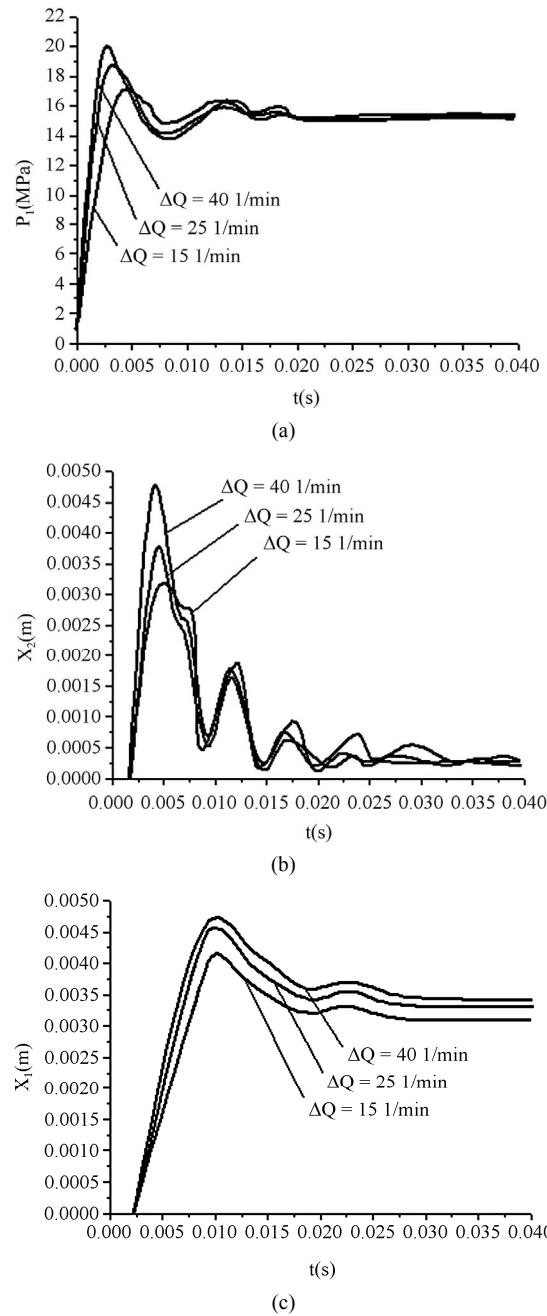


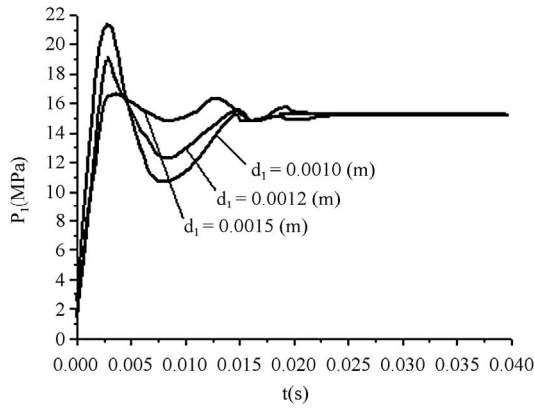
Figure 7. Simulation curves three.

and 0.10 cm (the thin curve) under the conditions that the initial oil pressure is 0.8 MPa, the setting pressure is 15 MPa and the step flow  $\Delta Q$  is 40 l/min.

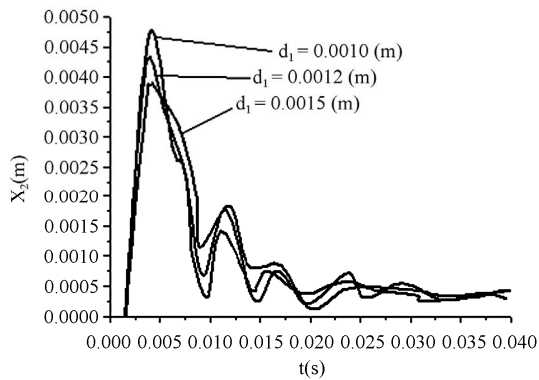
Figure 8 shows:

a)  $d_1$  has a great effect on the excessive pressure adjustment. The smaller  $d_1$ , the larger  $\Delta P_1$ . The response will be slower when  $d_1$  minifies.

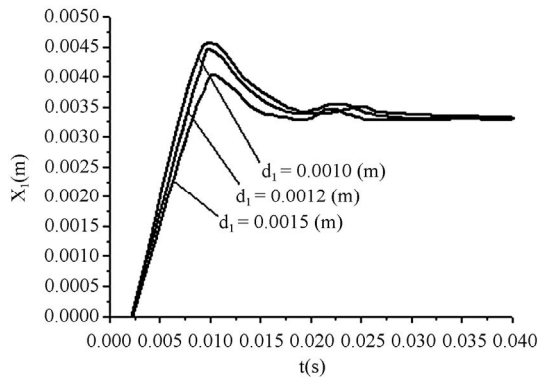
b) When  $d_1$  changes in a small area, it won't obviously affect the stability of the valve. When  $d_1$  minifies, the pilot valve core will close for a long time. If  $d_1$  increases appropriately, the  $\Delta P_1$  will decrease and the stability



(a)

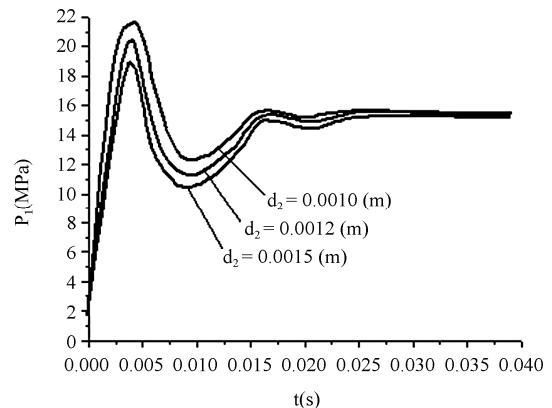


(b)

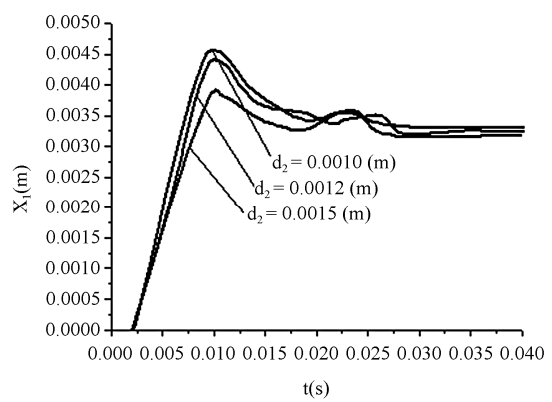


(c)

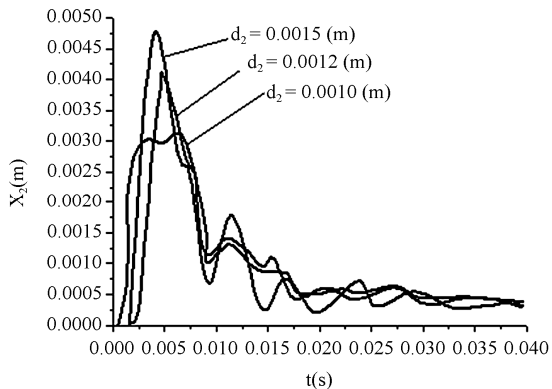
Figure 8. Simulation curves four.



(a)



(b)



(c)

Figure 9. Simulation curves five.

won't get worse.

5) Changes of damping orifice of the pilot valve seat.

The curves shown in **Figures 9(a)-(c)** are respectively the characteristic curves of the inlet port oil pressure, the pilot valve core and directional valve core displacement under the conditions that the initial oil pressure is 0.8 MPa, the setting pressure is 15 MPa and the step flow  $\Delta Q$  is 40 l/min when the diameters of the pilot valve damping orifice is respectively 0.15, 0.12 and 0.10 cm.

It is clear in **Figure 9** that  $d_2$  has an obvious effect on the dynamic characteristics of the valve. When  $d_2$  de-

creases to 0.10 cm, the oscillation phenomenon will hardly occur. However,  $\Delta P_1$  will correspondingly increase and the time of pressure peak will also have a little increase.

The above discussion shows that  $d_1$  and  $d_2$  not only affect the dynamic characteristics of the valve, but also have a certain match. Selecting  $d_1$  and  $d_2$  reasonably, the less overshoot of pressure can be gotten and the oscillation of the pilot valve core doesn't appear. **Figure 10** shows that the dynamic characteristics of the valve are satisfactory when  $d_1$  is 0.1 cm,  $d_2$  is 0.10 cm and the

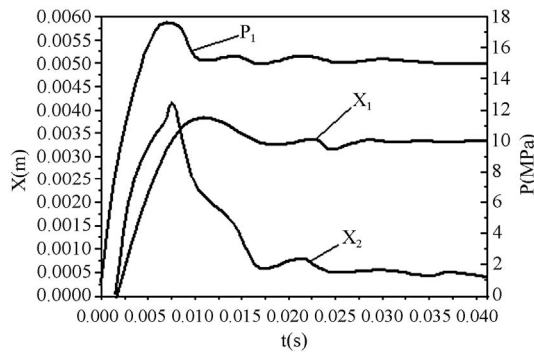


Figure 10. Simulation curves six.

other conditions are the same as Figures 8 and 9.

6) Effects of duct stiffness on the valve dynamic characteristics.

The duct's stiffness depends on the elastic modulus of the fluid and pipe. When the fluid modulus  $\beta_e$  is  $1.2 \times 10^8$  N/m<sup>2</sup>,  $9 \times 10^8$  N/m<sup>2</sup>,  $7 \times 10^9$  N/m<sup>2</sup> and the pipe between the pump and the distribution valve is flexible, the fluid capacitance of the pipe  $C_C$  is respectively 0.067, 0.114 and 0.199. The curves shown in Figures 11(a)-(c) are respectively the response curves of the inlet port oil pressure, the pilot valve core and directional valve core displacement under the conditions that the initial oil pressure  $P_0$  is 0.8 MPa, the setting pressure  $P^*$  is 15 MPa and the step flow  $\Delta Q$  is 40 l/min when  $C_C$  is respectively 0.067, 0.144 and 0.199.

The simulation results show:

a) With the increase of  $C_C$ , the vibration amplitude of the pilot valve falls. The excessive pressure adjustment  $\Delta P_1$  falls drastically but the transition time becomes longer, which is caused by the falling of the pipe's stiffness after the increase of fluid capacitance.

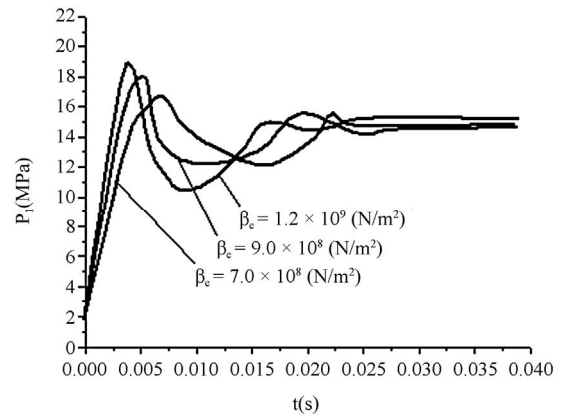
b) Flexible pipes can absorb the shock wave but the use of the flexible pipes will reduce the sensitivity of the valve, which must be considered in practical use.

7) Effects of the spring stiffness on the dynamic characteristics of valve.

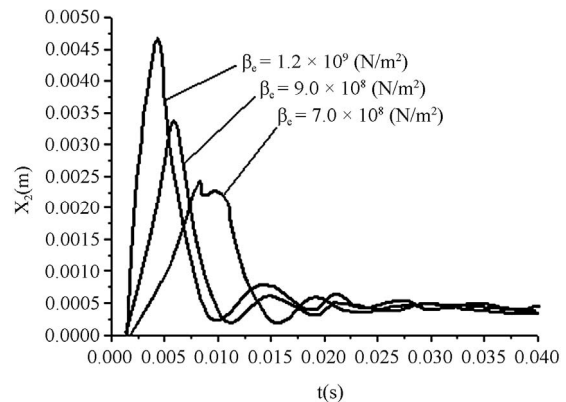
The results of digital simulation show:

a) The balance spring stiffness  $K_{t1}$  of the directional valve hardly affect the dynamic performance of the valve. Thus, the selection of  $K_{t1}$  is mainly in accordance with the static performance requirements (meeting the constant pressure accuracy).

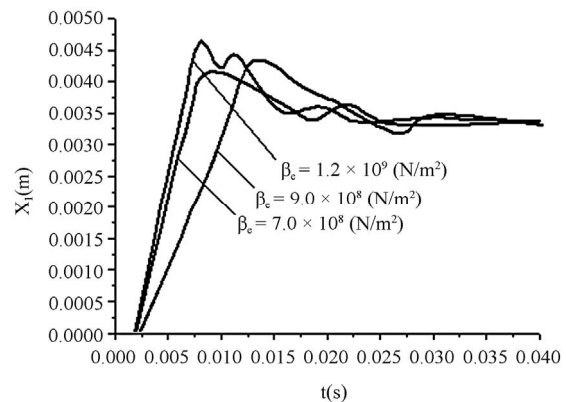
b) The balance spring stiffness  $K_{t2}$  of the pilot valve has a certain effect on the dynamic characteristics of the valve. With the falling of  $K_{t2}$ , the stability of the pilot core will be a little worse. Thus, the increase of  $K_{t2}$  is good for the improvement of the stability of the pilot valve, but the effect is more inapparent than the effect caused by reducing the diameter of damping orifice of the pilot valve seat. In addition, considering from the requirements of improving the static performance,  $K_{t2}$



(a)



(b)



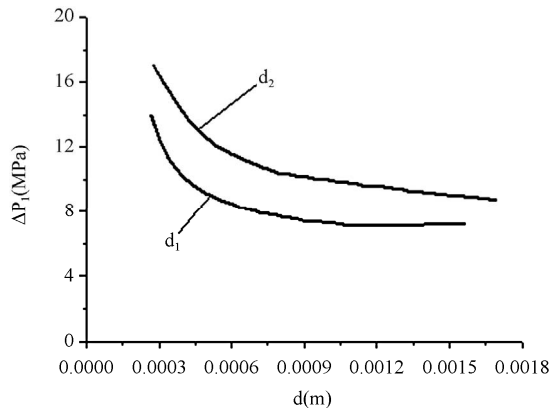
(c)

Figure 11. Simulation curves seven.

should be reduced in order to improve regulation precision. Therefore, the static performance is the main basis for selecting  $K_{t2}$ .

The curves on the excessive pressure adjustment  $\Delta P_1$ , peak time  $t_r$  and transition process time  $t_s$  change with the parameters are shown in Figures 12 and 14 according to the simulation results. It is shown in Figure 12 that  $\Delta P_1$  increases with the falling of  $d_1$  and  $d_2$ . It is shown in Figure 13 that the peak time  $t_r$  decreases with the increase of  $d_1$ ; the change of  $t_r$  is slow when  $d_1$  increases to a certain

value, then  $d_1$  increases slightly; the peak time  $t_s$  decreases with the increase of  $d_1$ ; when  $d_1$  is 0.001,  $t_s$  is the smallest; when  $d_1$  continues to increase,  $t_s$  will increase. It is shown in **Figure 14** that the variational trend of the peak time  $t_r$  with  $d_2$  is the same as that of  $d_1$ , but the change of  $t_r$  is a little slow.



**Figure 12.** Influence of the changes of  $d_1$  and  $d_2$  on  $\Delta P_1$ .

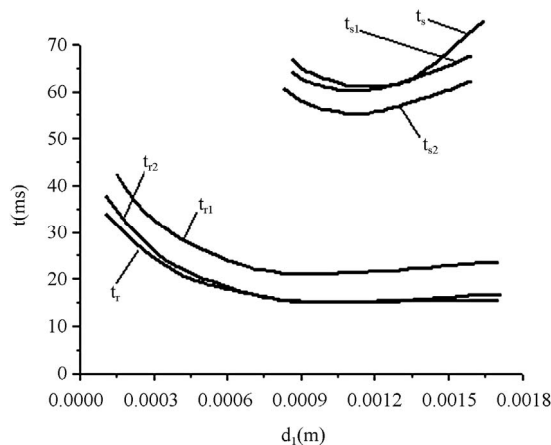


**Figure 13.** Influence of the changes of  $d_1$  on the response time.

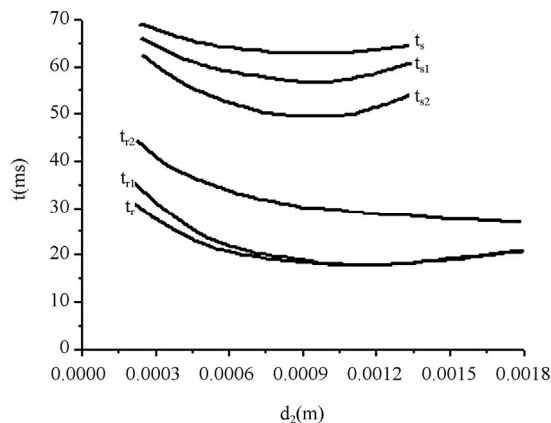


**Figure 14.** Influence of the changes of  $d_2$  on the response time.

## 6. Conclusions

Through the above analysis, the conclusions are as follows:

- 1) When the diameter of the directional valve damping orifice decreases, the pressure overshoot and peak time will increase.
- 2) The changes of the setting pressure  $P$  and the mass of the directional valve core and the directional valve right chamber volume  $V$  have little influence on the dynamic quality.
- 4) The pipeline volume has much influence on the dynamic quality.
- 5) To conclude the above, the curves of the distribution valve in the transitional process show that the vibration of the pilot valve affects the commutation, which causes the distribution valve to vibrate.
- 6) The balance spring stiffness of the directional valve and the balance spring stiffness of the pilot valve can be decided by the static characteristics of the valve.

## REFERENCES

- [1] G. P. Yang and C. P. Liang, "A Research on the New Hydraulic Impactor Control System," 2010 *International Conference on Measuring Technology and Mechatronics Automation*, Changsha, 13-14 March 2010, pp. 291-293.
- [2] G. P. Yang, L. H. Chen and H. Huang, "The Research of a Full Hydraulic Pressure Hydraulic Impactor with Strike Energy and Frequency Adjusted Independently," *The 6th International Conference on Fluid Power Transmission and Control*, Hangzhou, 1-5 September 2005, pp. 262-265.
- [3] G. P. Yang, "Research of a Full Hydraulic Pressure Hydraulic Impactor with Strike Energy and Frequency Adjusted Independently," *Journal of Hunan University of Science & Technology (Natural Science Edition)*, Vol. 21, No. 1, 2006, pp. 25-28.
- [4] G. P. Yang, "Research on Design Theory on the Return Oil Chamber of a New Hydraulic Impactor," *China Journal of Highway and Transport*, Vol. 15, No. 1, 2002, pp. 113-115.
- [5] X. B. Yang and G. P. Yang, "The Research of a Pressure Feedback Full Hydraulic Pressure Hydraulic Impactor with Strike Energy and Frequency Adjusted Independently," *China Mechanical Engineering*, Vol. 13, No. 23, 2002, pp. 2044-2047.
- [6] G. P. Yang, "Research on Computer Simulation for a New Pilot Type Hydraulic Impactor System," *Mechanical Science and Technology*, Vol. 25, No. 2, 2006, pp. 233-237.
- [7] G. P. Yang, F. L. Zhu and G. J. Long, "Research on Design Theory on the Return Oil Chamber of a New Hydraulic Impactor," *China Mechanical Engineering*, No. 12, 2003, pp. 1062-1065.
- [8] G. P. Yang, J. H. Gao and B. Chen, "Computer Simulation of Controlled Hydraulic Impactor System," *Ad-*

*vanced Materials Research (Materials Science and Engineering)*, Vol. 179-180, 2011, pp. 122-127.

- [9] G. P. Yang, B. Chen and J. H. Gao, "Improved Design and Analysis of Hydraulic Impact Hammer Based on Virtual Prototype Technology," *Applied Mechanics and Materials (Measuring Technology and Mechatronics Automation)*, Vol. 48-49, 2011, pp. 607-610.

[doi:10.4028/www.scientific.net/AMM.48-49.607](https://doi.org/10.4028/www.scientific.net/AMM.48-49.607)

- [10] G. P. Yang, "The Application of Stress Wave Theory in Concrete Impact Crushing," *China Journal of Highway and Transport*, Vol. 6, No. 2, 2000, pp. 124-126.

## Appendix

**Table type styles (Table caption is indispensable).**

Sign	Meaning	Reference Value	Unit
P <sub>2</sub>	left chamber pressure of the directional valve	middle variable	Pa
P <sub>3</sub>	front chamber pressure of the pilot valve	middle variable	Pa
d <sub>0</sub>	diameter of the directional valve core	$2.0 \times 10^{-2}$	m
d <sub>3</sub>	diameter of the pilot valve orifice	$4 \times 10^{-3}$	m
d <sub>1</sub>	diameter of the directional valve damping orifice	$1.2 \times 10^{-3}$	m
d <sub>2</sub>	diameter of the pilot valve damping orifice	$1.5 \times 10^{-3}$	m
l <sub>1</sub>	length of the directional valve damping orifice	$8.0 \times 10^{-3}$	m
l <sub>2</sub>	length of pilot valve damping orifice	$4.0 \times 10^{-3}$	m
$\alpha_1$	half-cone angle of the pilot valve core	20	°
A <sub>0</sub>	side area of the front and back chamber of the directional valve	$6.12 \times 10^{-4}$	m <sup>2</sup>
A <sub>3</sub>	area of the pilot valve seat orifice	$0.126 \times 10^{-4}$	m <sup>2</sup>
X <sub>1</sub>	displacement of the directional valve	variable	m
X <sub>11</sub>	pre-compression of the directional valve spring	$0.80 \times 10^{-3}$	m
X <sub>2</sub>	displacement of the pilot valve displacement	variable	m
X <sub>12</sub>	pre-compression of the pilot valve spring	$0.90 \times 10^{-3}$	m
X <sub>3</sub>	displacement of the piston	variable	m
K <sub>11</sub>	spring stiffness of the directional valve	$1.98 \times 10^{-3}$	N/m
K <sub>12</sub>	spring stiffness of the pilot valve	$2.44 \times 10^{-3}$	N/m
m <sub>1</sub>	equivalent mass of the directional valve core and spring	$1.263 \times 10^{-4}$	N·S <sup>2</sup> /m
m <sub>2</sub>	equivalent mass of the pilot valve core and spring	$6.263 \times 10^{-6}$	N·S <sup>2</sup> /m
B <sub>1</sub>	movement damping coefficient of the directional valve core	$0.96 \times 10^{-1}$	N·S/m
B <sub>2</sub>	movement damping coefficient of the pilot valve core	$1.4 \times 10^{-3}$	N·S/m
V <sub>1</sub>	total volume of the directional valve left chamber and duct	$6.578 \times 10^{-4}$	m <sup>3</sup>
V <sub>2</sub>	volume of the right chamber of the directional valve	$1.12 \times 10^{-5}$	m <sup>3</sup>
V <sub>3</sub>	front chamber volume of the pilot valve	$0.15 \times 10^{-6}$	m <sup>3</sup>
L <sub>1</sub>	length of the control volume of the pilot valve chamber	$0.8 \times 10^{-2}$	m
$\rho$	oil density	$9.0 \times 10^3$	N/m <sup>3</sup>
$\nu$	oil kinematic viscosity	$4.0 \times 10^{-5}$	m <sup>2</sup> /s
Q <sub>d</sub>	flow rate of the system pump	40	l/min
Q <sub>s</sub>	relief-flow of the reversing valve	Q <sub>s</sub> = 0.1% Q <sub>d</sub> = 4	l/min
K	oil bulk modulus of elasticity	$6.0 \times 10^8$	N/m <sup>2</sup>
C <sub>d1</sub>	flow coefficient of the pilot valve orifice		Non-dimensional
C <sub>e1</sub>	correction coefficient of the initial segment of the laminar flow of the directional valve damping orifice		Non-dimensional
C <sub>e2</sub>	correction coefficient of the initial segment of the laminar flow of the pilot valve damping orifice		Non-dimensional
C <sub>v1</sub>	velocity coefficient of the pilot valve orifice		Non-dimensional